Frustrated Magnetism of Dipolar Molecules on a Square Optical Lattice: Prediction of a Quantum Paramagnetic Ground State

Haiyuan Zou,[1,2] Erhai Zhao,[3] and W. Vincent Liu[1,2,4]

[1]*Wilczek Quantum Center, School of Physics and Astronomy and T. D. Lee Institute, Shanghai Jiao Tong University, Shanghai 200240, China*

[2]*Department of Physics and Astronomy, University of Pittsburgh, Pittsburgh, Pennsylvania 15260, USA*

[3]*Department of Physics and Astronomy, George Mason University, Fairfax, Virginia 22030, USA*

[4]*Center for Cold Atom Physics, Chinese Academy of Sciences, Wuhan 430071, China*

(Received 2 March 2017; published 31 July 2017)

Motivated by the experimental realization of quantum spin models of polar molecule KRb in optical lattices, we analyze the spin 1/2 dipolar Heisenberg model with competing anisotropic, long-range exchange interactions. We show that, by tilting the orientation of dipoles using an external electric field, the dipolar spin system on square lattice comes close to a maximally frustrated region similar, but not identical, to that of the J_1-J_2 model. This provides a simple yet powerful route to potentially realize a quantum spin liquid without the need for a triangular or kagome lattice. The ground state phase diagrams obtained from Schwinger-boson and spin-wave theories consistently show a spin disordered region between the Néel, stripe, and spiral phase. The existence of a finite quantum paramagnetic region is further confirmed by an unbiased variational ansatz based on tensor network states and a tensor renormalization group.

DOI: 10.1103/PhysRevLett.119.050401

Understanding highly entangled quantum matter remains a challenging goal of condensed matter physics [1]. One paradigmatic example is quantum spin liquids in frustrated spin systems which defy any conventional long range order characterized by broken symmetry at zero temperature [1–3]. Instead, the ground state features long-range entanglement and nonlocal excitations. Spin liquids are also fertile ground for studying quantum phases described by gauge field theories and topological order [4]. While the existence of spin liquids has been firmly established in a number of exactly solvable models, e.g., the toric code [5] or the honeycomb Kitaev model [6], the nature of the ground states for many frustrated spin models, e.g., the Heisenberg model on kagome lattices or the J_1-J_2 model on square lattices, still remains controversial despite the great theoretical progress in recent years [7–11]. An unambiguous experimental identification of quantum spin liquids in solid state materials also seems elusive [1]. It is, then, important to explore new physical systems that can cleanly realize well-defined spin models which have potential spin liquid ground states.

Recent breakthrough experiments on magnetic atoms [12] and polar molecules [13,14] confined in deep optical lattices introduced a new class of lattice spin models with competing exchange interactions that are long-ranged and anisotropic. The resulting spin Hamiltonians, such as the dipolar XXZ and dipolar Heisenberg models, are highly tunable by the external fields that couple to the magnetic and electric dipoles [15,16]. Here, we show that these models on square lattices feature strong exchange (not geometric) frustration and a quantum paramagnetic ground state for intermediate dipole tilting angles. This claim is consistently supported by physical arguments, two independent semiclassical analytical methods, and full numerical calculation based on a tensor network ansatz [17–21]. Our key insight is that spin liquids may arise naturally from the system of tilted, interacting dipoles on square lattices, without the requirement of peculiar (e.g., triangular or kagome) lattices or exotic (e.g., Kitaev or ring-exchange) interactions.

The dipolar XXZ and Heisenberg model.—First, we define the dipolar XXZ model on a square optical lattice

$$H_{XXZ} = \frac{J}{2}\sum_{i\neq j} f(\mathbf{r}_i - \mathbf{r}_j)(S_i^x S_j^x + S_i^y S_j^y + \eta S_i^z S_j^z). \quad (1)$$

Here, i and j label the lattice sites, $\mathbf{S}_i = (S_i^x, S_i^y, S_i^z)$ are the spin (or pseudospin) operators at site i, and η is the exchange anisotropy. The key new feature here is that the coupling between the two spins depends on their relative position $\mathbf{r} = \mathbf{r}_i - \mathbf{r}_j$ and the external field (dipole) direction $\hat{\boldsymbol{d}}$

$$f(\mathbf{r}) = [1 - 3(\hat{\boldsymbol{r}}\cdot\hat{\boldsymbol{d}})^2](a/r)^3, \quad (2)$$

with a the lattice constant [Fig. 1(a)]. This geometric factor, characteristic of the dipole-dipole interaction, dictates that spin interactions are long-ranged and anisotropic. For the special case of $\eta = 1$, H_{XXZ} reduces to the dipolar Heisenberg model

$$H_d = \frac{J}{2}\sum_{i\neq j} f(\mathbf{r}_i - \mathbf{r}_j)\mathbf{S}_i\cdot\mathbf{S}_j, \quad (3)$$

and for $\eta = 0$, it reduces to the dipolar XY model, H_{XY}.

 © 2017 American Physical Society

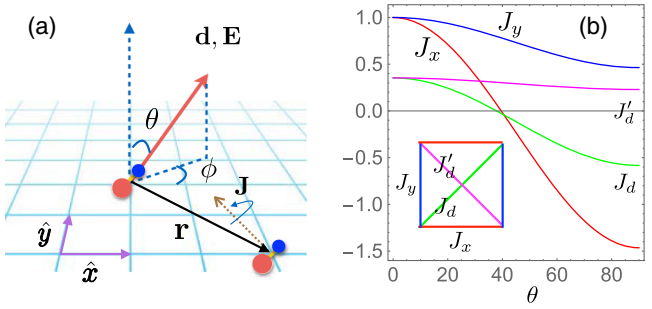

FIG. 1. (a) Dipolar molecules such as KRb confined in a square optical lattice. The direction of the dipoles $\mathbf{d}$ is tuned by the electric field $\mathbf{E}$. Two rotational states of the molecules play the role of pseudospin up and down. The system is described by the effective XXZ model Eq. (1). With the proper choice of E, it reduces to the dipolar Heisenberg model H_d in Eq. (3). (b) Leading exchange interactions J_x, J_y, J_d, and J'_d (inset) as functions of the dipole tilting angle θ for fixed $\phi = 25°$. Strong frustration occurs at intermediate θ.

Spin models of the form of H_{XXZ} have been realized experimentally in two settings. In Ref. [12], the spin dynamics of a gas of ^{52}Cr atoms in optical lattices was observed. Each Cr atom carries a magnetic moment of $7\mu_B$ and hyperfine spin $S = 3$. An external magnetic field is used to align the magnetic dipoles in the direction of $\hat{\boldsymbol{d}}$. Such a dipolar gas of Cr in a deep lattice is shown to be described by H_{XXZ} with $J = -\mu_0(g\mu_B)^2/4\pi a^3 < 0$ and $\eta = -2$ [12]. Note that J induced by the dipolar interaction is, contrary to the superexchange, independent of the tunneling, and it can be set as the unit of energy.

Polar molecules such as ^{87}Rb confined in optical lattices with negligible tunneling provide another way to realize H_{XXZ} with $S = 1/2$ and tunable J and η [13]. Each molecule carries an electric dipole moment $\mathbf{d}$ and undergoes rotation with angular momentum $\mathbf{J}$ [see Fig. 1(a)]. Here, the pseudospin $1/2$ refers to two rotational states of the molecule labeled by $|j, m\rangle$, where j is the quantum number of the rotational angular momentum $\mathbf{J}$ and m is its projection onto the quantization axis, chosen as the direction of the external electric field E. More details can be found in Ref. [13,16,22]. The dipole-dipole interaction projected onto the sub-Hilbert space of the pseudospins then takes the form of a spin Hamiltonian, where the spin flips correspond to transitions between the rotational states. For example, by choosing $|j, m\rangle = |0, 0\rangle$ and $|1, 0\rangle$ as the pseudospin down and up, respectively, Refs. [16,22] showed that the system is described by the effective Hamiltonian H_{XXZ} with $J = D_t^2/2\pi\epsilon_0 a^3 > 0$ and $\eta = (D_1 - D_0)^2/2D_t^2 > 0$. Here, the dipole matrix element $D_t = \langle 1,0|d^0|0,0\rangle$, $D_1 = \langle 1,0|d^0|1,0\rangle$, $D_0 = \langle 0,0|d^0|0,0\rangle$, and d^0 together with $d^\pm$ form the vector dipole operator in the spherical basis [16,22].

The anisotropy η increases monotonically with E. As shown in Ref. [16], when $E \simeq 1.7B/|\mathbf{d}|$ with B the energy splitting of the two pseudospin states, $\eta = 1$, and one arrives at the dipolar Heisenberg model H_d. In the KRb experiment [13] carried out at zero field and cubic lattice, $\eta \to 0$, the dipolar XY model H_{XY} was realized with J on the order of 100 Hz. Despite the low filling factor and high entropy, coherent spin dynamics was observed via Ramsey spectroscopy [13] and modeled theoretically in Ref. [14]. Recently, Yao *et al.* [16] considered general η and worked out the phase diagram of H_{XXZ} on the Kagome and triangular lattice using Density Matrix Renormalization Group (DMRG). For both lattices, they found evidence for quantum spin liquid centering around the Heisenberg limit, $\eta = 1$ and $\theta = 0$, in which θ is defined by $\hat{\boldsymbol{d}} \cdot \hat{\boldsymbol{x}} = \sin\theta\cos\phi$ with $\hat{\boldsymbol{x}}$ representing a base vector of the square lattice. Thus, the physics is connected to a geometrically frustrated Heisenberg model on both lattices, with additional longer range interactions and anisotropy η.

In this Letter, we study the phases of H_d on a square lattice as the dipoles are tilted towards the lattice plane [see Fig. 1(a)] for $S = 1/2$ and $J > 0$. We show that strong frustration occurs at intermediate dipole tilting angle θ, leading to a quantum paramagnetic ground state. We emphasize that, here, the frustration is not imposed by the lattice geometry, but instead, is due to the competition between the exchange interactions, analogous to the J_1-J_2 model. Relatedly, the quantum paramagnetic phase appears at intermediate θ values (not around $\theta = 0$ as in Ref. [16]) between the Néel and the stripe orders. Thus, it differs qualitatively from the spin liquids studied in Ref. [16]. We will also employ different methods to solve the dipolar quantum spin models.

Competing exchanges for tilted dipoles.—To appreciate the possible phases of H_d as $\hat{\boldsymbol{d}}$ is tuned as well as its connection to frustrated quantum spin models [3,23], let us consider the leading exchange couplings between the nearest neighbors, $J_x = Jf(a\hat{\boldsymbol{x}})$ and $J_y = Jf(a\hat{\boldsymbol{y}})$, and the next nearest neighbors, $J_d = Jf(a\hat{\boldsymbol{x}} + a\hat{\boldsymbol{y}})$ and $J'_d = Jf(a\hat{\boldsymbol{x}} - a\hat{\boldsymbol{y}})$ [Fig. 1(b)]. Their relative magnitudes and signs depend sensitively on the dipole tilting angle θ and ϕ. One example is shown in Fig. 1(b) for fixed $\phi = 25°$. At small θ, $J_x \sim J_y$ dominates because it is about three times that of $J_d \sim J'_d$. The situation is reminiscent of the J_1-J_2 model in the regime of the Néel order. As θ is increased, J_d and J'_d grow relative to J_x and J_y. The system becomes more frustrated due to the increased competition of the exchanges. This is the most interesting parameter region. Around $\theta \simeq 40°$, J_x and J_d vanish while $J'_d \sim 0.4J_y$. The model can be viewed as coupled Heisenberg chains. For even larger θ, J_x and J_d switch signs to become ferromagnetic, and the stripe order is expected. Clearly, the physics of H_d is much richer than the J_1-J_2 model. In fact, the two models only overlap at one single point, $\theta = \phi = 0$, where $J_2/J_1 = 1/2\sqrt{2} \approx 0.35$ and the system is Néel ordered.

The degree of frustration can be measured by the "spin gap" Δ, the energy difference between the ground and the

first excited state, from exact diagonalization of H_d for a 4×4 lattice [24]. For example, we observe a pronounced peak in Δ around $\theta \sim 28°$ for $\phi = 25°$, which indicates strong frustration and points to a gapped, spin disordered ground state [25]. For fixed $\phi = 35°$, the spin structure factor shows a clear peak at (π, π) for $\theta \sim 15°$ for the Néel order, a peak at $(0, \pi)$ for $\theta \sim 50°$ for the stripe order, but no well defined peaks around $\theta \sim 35°$, consistent with the argument above.

Spin-wave and Schwinger-boson theory.—First, we obtain a coarse phase diagram of H_d on the (θ, ϕ) plane using two widely adopted analytical methods in frustrated quantum magnetism. This will help identify the interesting regions for the more expensive tensor network calculations to focus on. The starting point is the classical solution of H_d by the Luttinger-Tisza method [26]. H_d is of the form $\sum_{ij} J_{ij} \mathbf{S}_i \cdot \mathbf{S}_j$ with hard spin constraint $\mathbf{S}_i = S$ and J_{ij} only depends on $\mathbf{r}_i - \mathbf{r}_j$. A theorem states that the classical ground state is a planar spin spiral, $\mathbf{S}_\mathbf{r}/S = \hat{\boldsymbol{x}} \cos(\mathbf{Q} \cdot \mathbf{r}) + \hat{\boldsymbol{y}} \sin(\mathbf{Q} \cdot \mathbf{r})$ with an ordering wave vector $\mathbf{Q} = (Q_x, Q_y)$ [27]. The classical phase diagram [24] consists of three phases. The first is the Néel order corresponding to $\mathbf{Q} = (\pi, \pi)$ for small θ. The second is the stripe phase with $\mathbf{Q} = (0, \pi)$ for large θ but not too large ϕ. These two spin orders are collinear. The third, spiral phase fills the rest of the phase diagram, for large θ and ϕ, where $\mathbf{Q}$ varies continuously and, in general, is incommensurate with the lattice.

Beyond the classical limit, quantum fluctuations will suppress the magnetic order and shift the phase boundary. These effects can be described qualitatively by modified spin wave theory [28–30]. In the Holstein-Primakoff representation, we expand H_d in a series of $1/S$ and keep up to the quartic order of bosonic operators, i.e., we take into account the interactions between the linear spin waves. The bosonic Hamiltonian is solved by self-consistent mean field theory [24]. The result is summarized in Fig. 2(a). We find that the phase boundary of the Néel (stripe) phase moves towards smaller (larger) θ values, opening up an intermediate region in between where the magnetization vanishes. The spiral phase also recedes to higher ϕ values. We label this quantum paramagnetic region with QP. This is precisely the region where the various exchanges compete and the system is most frustrated.

Alternatively, we can take into account quantum fluctuations by the rotationally invariant Schwinger boson mean field theory which is nonperturbative in S [31,32]. It is a well tested method capable of describing both magnetically ordered and spin liquid states of frustrated spin models [33–36]. The resulting phase diagram is shown in Fig. 2(b). Here, each magnetic order corresponds to condensation of bosons at a certain wave vector $\mathbf{Q}$. Within a finite strip region labeled by QP between the Néel and stripe phase, the condensation fraction vanishes and the spin excitations are gapped, corresponding to a quantum paramagnetic phase. The fact that two different approximations agree on the existence of QP indicates that it must be a robust feature of the model H_d.

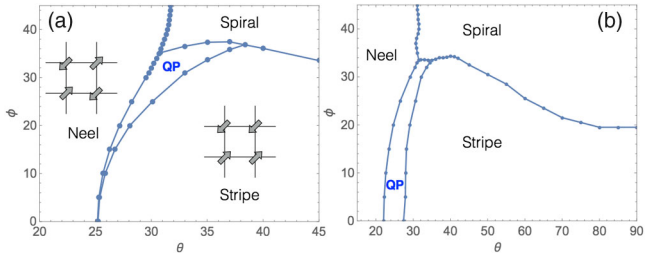

FIG. 2. Phase diagram of H_d from (a) modified spin wave theory and (b) Schwinger boson mean field analysis. Both methods reveal a QP phase amidst the three long ranged ordered phases: Néel, stripe, and spiral.

Phase diagram from a tensor network ansatz.—A variational ansatz based on tensor network states [17–19] has recently emerged as an accurate and unbiased algorithm for solving two dimensional frustrated quantum spin models [11,37–39]. In this approach, the ground state many-body wave function $|\Psi\rangle$ is constructed from a network of tensors T_i defined on lattice site i: $|\Psi\rangle = \mathrm{tr} \prod_i T_i$, where tr stands for contraction of neighboring tensors. Each tensor T_i has four virtual legs (indices), each with bond dimension D designed to build up the quantum entanglement between lattice sites, and one physical leg representing the spin. We choose a $L \times L$ cluster as the unit cell with periodic boundary conditions. The algorithm starts with L^2 random tensors, and imaginary time evolution is used to update the local tensors, $|\psi'\rangle = \exp(-\tau H)|\psi\rangle$, until convergence is achieved. We adopt the simple update scheme [40] based on singular value decomposition. By using the Trotter-Suzuki formula $\exp(-\tau H) \approx \prod_{i=1}^{4} \exp(-\tau H_i) + O(\tau^2)$, each iteration of projection for one plaquette can be done using $\exp(-\tau H_i)$ $(i = 1, 2, 3, 4)$ in four separate steps, in which each step evolves three sites (a right triangle) in one plaquette with H_i contains only three terms of the Hamiltonian. For example, $H_{1,2}$ contains J_x, J_y, and J_d terms and $H_{3,4}$ contains J_x, J_y, and J'_d terms (See Refs. [11,24,41,42]).

The expectation value of a local operator O_j at site j, $\langle O_j \rangle = \langle \Psi | O_j | \Psi \rangle / \langle \Psi | \Psi \rangle$, can be computed by tensor contraction, $\langle O_j \rangle = \mathrm{tr}(\mathcal{O}_j \prod_{i \neq j} \mathcal{T}_i)/\mathrm{tr} \prod_i \mathcal{T}_i$ where $\mathcal{T}_i = T_i^\dagger T_i$ and $\mathcal{O}_j = T_j^\dagger O_j T_j$. We evaluate it using an iterative, real space coarse-graining procedure known as the tensor renormalization group which enables one to reach the thermodynamic limit [20,21]. In this way, we calculate order parameters such as magnetization $M = \sqrt{\langle S_x \rangle^2 + \langle S_y \rangle^2 + \langle S_z \rangle^2}$ [24].

With increasing D, quantum fluctuations beyond spin wave or Schwinger boson analysis are taken into account.

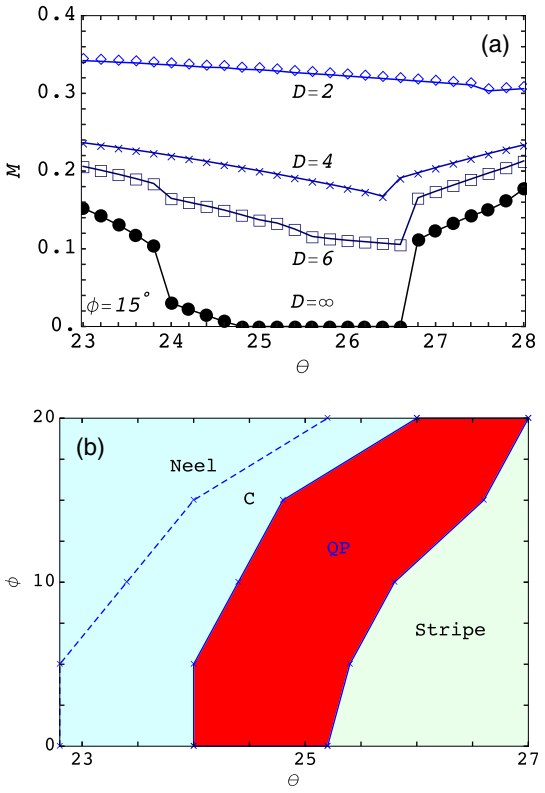

FIG. 3. (a) The magnetizations M as functions of θ for fixed $\phi = 15°$ and increasing $D = 2, 4, 6$. Extrapolation to infinite D by fitting M in polynomials of $1/D$ shows that the magnetic order parameters are suppressed in a finite region of θ, indicating a quantum paramagnetic phase. At $\theta = 24.0°$, a sudden drop of M occurs inside the Néel phase. (b) Phase diagram of H_d for $\phi \leq 20°$ obtained from the tensor network ansatz showing a spin-disordered, QP phase sandwiched between the Néel and stripe phases, broadly consistent with Fig. 2. Region C still has the Néel order, the dashed line indicates where the magnetization M drops suddenly.

The suppression of M is illustrated in Fig. 3(a) for different D values at fixed $\phi = 15°$. By extrapolating the results to infinite D, we can determine the phase boundary of the Néel and stripe phases. Repeating the procedure for different ϕ values, we obtain the phase diagram Fig. 3(b). It firmly establishes the existence of a finite quantum paramagnetic region (in red), about one degree wide in θ and persisting from $\phi = 0$ up to $\phi = 20°$, where the magnetization is completely suppressed to zero. The paramagnetic phase is narrower than the prediction of the Schwinger boson mean field theory which tends to overestimate the spin disordered region. Inside the Néel phase, there is a sudden drop of M. Note that the spiral phase, in general, is incompatible with the $L \times L$ cluster choice, even for large L. So we refrain from carrying out the tensor network ansatz beyond $\phi = 20°$. On the other hand, our numerics indicates that the phase boundary presented in Fig. 3(b) is not expected to depend sensitively on L as it varies [24]. Finally, we point out that the quantum paramagnetic phase is a robust feature of the dipolar XXZ model. It persists when η is tuned away from the Heisenberg limit, e.g., down to $\eta = 0.5$ [24].

It is challenging to pin down the precise nature of the paramagnetic phase found here in the dipolar Heisenberg model. Similar difficulties also arise for the J_1-J_2 model where the latest DMRG result [10] suggests that the paramagnetic region may consist of a subregion with a plaquette valence bond solid (VBS) order and a second, spin liquid or quantum critical region. Possible spin liquid states for the J_1-J_2 model on square lattices have been classified within the framework of the Schwinger boson mean field theory [36]. Yet it remains unclear which one is realized in the ground state. It is possible that the QP region of H_d may contain some VBS order. Unlike the J_1-J_2 model, the C_4 rotation symmetry is broken in H_d as soon as the dipoles are tilted, which may disfavor the plaquette VBS. Because of the limitation of the cluster size, we could not accurately compute the dimer correlation functions. Future numerical work with larger L and D is required to shed light on this open issue. The new formulation of symmetric tensor networks [43,44] and Lanczos iteration [45] seems promising to detect the possible topological order and accessing the excitation spectrum.

In summary, we presented consistent evidence that a quantum paramagnetic phase emerges from the simple physical system of interacting, tilted dipoles confined on square optical lattices. Our analysis of the dipolar Heisenberg model for general (θ, ϕ) adds a new dimension to frustrated quantum magnetism. It allows the exploration of potential spin liquids beyond the J_1-J_2 model which has not been realized cleanly so far. For KRb, J is about 100 Hz, or 5 nK, similar to the superexchange scale t^2/U of the Fermi Hubbard model recently studied using a quantum gas microscope [46–50]. Thus, it seems possible to probe the spin order or spin correlations of H_d and related models in future experiments.

We thank Ying-Jer Kao, Bo Liu, Jaime Merino, and Ling Wang for helpful discussions. This work is supported by the U.S. AFOSR Grants No. FA9550-16-1-0006 (H. Z., E. Z., and W. V. L.), No. NSF PHY-1205504 (E. Z.), and ARO Grant No. W911NF-11-1-0230, the Chinese National Science Foundation through the Overseas Scholar Collaborative Program (Grant No. 11429402) sponsored by Peking University and another Grant (No. 11227803), and the Strategic Priority Research Program of the Chinese Academy of Sciences (Grant No. XDB21010100) (W. V. L.). Part of the simulations were done at the supercomputing resources provided by the University of Pittsburgh Center for Simulation and Modeling.

[1] L. Savary and L. Balents, Rep. Prog. Phys. **80**, 016502 (2017).
[2] Y. Zhou, K. Kanoda, and T.-K. Ng, Rev. Mod. Phys. **89**, 025003 (2017).

[3] H. Diep, *Frustrated Spin Systems* (World Scientific, Singapore, 2013).
[4] X.-G. Wen, Phys. Rev. B **65**, 165113 (2002).
[5] A. Kitaev, Ann. Phys. (Amsterdam) **303**, 2 (2003).
[6] A. Kitaev, Ann. Phys. (Amsterdam) **321**, 2 (2006).
[7] S. Yan, D. A. Huse, and S. R. White, Science **332**, 1173 (2011).
[8] Y. Iqbal, F. Becca, S. Sorella, and D. Poilblanc, Phys. Rev. B **87**, 060405 (2013).
[9] H.-C. Jiang, H. Yao, and L. Balents, Phys. Rev. B **86**, 024424 (2012).
[10] S.-S. Gong, W. Zhu, D. N. Sheng, O. I. Motrunich, and M. P. A. Fisher, Phys. Rev. Lett. **113**, 027201 (2014).
[11] L. Wang, Z.-C. Gu, F. Verstraete, and X.-G. Wen, Phys. Rev. B **94**, 075143 (2016).
[12] A. de Paz, A. Sharma, A. Chotia, E. Maréchal, J. H. Huckans, P. Pedri, L. Santos, O. Gorceix, L. Vernac, and B. Laburthe-Tolra, Phys. Rev. Lett. **111**, 185305 (2013).
[13] B. Yan, S. A. Moses, B. Gadway, J. P. Covey, K. R. A. Hazzard, A. M. Rey, D. S. Jin, and J. Ye, Nature (London) **501**, 521 (2013).
[14] K. R. A. Hazzard, B. Gadway, M. Foss-Feig, B. Yan, S. A. Moses, J. P. Covey, N. Y. Yao, M. D. Lukin, J. Ye, D. S. Jin, and A. M. Rey, Phys. Rev. Lett. **113**, 195302 (2014).
[15] A. V. Gorshkov, S. R. Manmana, G. Chen, J. Ye, E. Demler, M. D. Lukin, and A. M. Rey, Phys. Rev. Lett. **107**, 115301 (2011).
[16] N. Y. Yao, M. P. Zaletel, D. M. Stamper-Kurn, and A. Vishwanath, arXiv:1510.06403.
[17] F. Verstraete and J. I. Cirac, arXiv:cond-mat/0407066.
[18] J. Jordan, R. Orús, G. Vidal, F. Verstraete, and J. I. Cirac, Phys. Rev. Lett. **101**, 250602 (2008).
[19] P. Corboz, R. Orús, B. Bauer, and G. Vidal, Phys. Rev. B **81**, 165104 (2010).
[20] M. Levin and C. P. Nave, Phys. Rev. Lett. **99**, 120601 (2007).
[21] Z. Y. Xie, J. Chen, M. P. Qin, J. W. Zhu, L. P. Yang, and T. Xiang, Phys. Rev. B **86**, 045139 (2012).
[22] A. V. Gorshkov, S. R. Manmana, G. Chen, E. Demler, M. D. Lukin, and A. M. Rey, Phys. Rev. A **84**, 033619 (2011).
[23] L. Balents, Nature (London) **464**, 199 (2010).
[24] See Supplemental Material at http://link.aps.org/supplemental/10.1103/PhysRevLett.119.050401 for a detailed description.
[25] P. Sindzingre, Phys. Rev. B **69**, 094418 (2004).
[26] J. M. Luttinger and L. Tisza, Phys. Rev. **70**, 954 (1946).
[27] T. A. Kaplan and N. Menyuk, Philos. Mag. **87**, 3711 (2007).
[28] M. Takahashi, Phys. Rev. B **40**, 2494 (1989).
[29] D. Chu and J.-l. Shen, Phys. Rev. B **44**, 4689 (1991).
[30] S.-M. Cui, J. Phys. Condens. Matter **4**, L389 (1992).
[31] D. P. Arovas and A. Auerbach, Phys. Rev. B **38**, 316 (1988).
[32] N. Read and S. Sachdev, Phys. Rev. Lett. **66**, 1773 (1991).
[33] A. Mezio, C. N. Sposetti, L. O. Manuel, and A. E. Trumper, J. Phys. Condens. Matter **25**, 465602 (2013).
[34] J. Merino, M. Holt, and B. J. Powell, Phys. Rev. B **89**, 245112 (2014).
[35] S. B. Lee, J.-S. Jeong, K. Hwang, and Y. B. Kim, Phys. Rev. B **90**, 134425 (2014).
[36] X. Yang and F. Wang, Phys. Rev. B **94**, 035160 (2016).
[37] H. Zou, B. Liu, E. Zhao, and W. V. Liu, New J. Phys. **18**, 053040 (2016).
[38] S. Jiang, P. Kim, J. H. Han, and Y. Ran, arXiv:1610.02024.
[39] H. J. Liao, Z. Y. Xie, J. Chen, Z. Y. Liu, H. D. Xie, R. Z. Huang, B. Normand, and T. Xiang, Phys. Rev. Lett. **118**, 137202 (2017).
[40] H. C. Jiang, Z. Y. Weng, and T. Xiang, Phys. Rev. Lett. **101**, 090603 (2008).
[41] P. Corboz, J. Jordan, and G. Vidal, Phys. Rev. B **82**, 245119 (2010).
[42] P. Corboz and F. Mila, Phys. Rev. B **87**, 115144 (2013).
[43] S. Jiang and Y. Ran, Phys. Rev. B **92**, 104414 (2015).
[44] J.-W. Mei, J.-Y. Chen, H. He, and X.-G. Wen, Phys. Rev. B **95**, 235107 (2017).
[45] R.-Z. Huang, H.-J. Liao, Z.-Y. Liu, H.-D. Xie, Z.-Y. Xie, H.-H. Zhao, J. Chen, and T. Xiang, arXiv:1611.09574.
[46] M. F. Parsons, F. Huber, A. Mazurenko, C. S. Chiu, W. Setiawan, K. Wooley-Brown, S. Blatt, and M. Greiner, Phys. Rev. Lett. **114**, 213002 (2015).
[47] L. W. Cheuk, M. A. Nichols, M. Okan, T. Gersdorf, V. V. Ramasesh, W. S. Bakr, T. Lompe, and M. W. Zwierlein, Phys. Rev. Lett. **114**, 193001 (2015).
[48] M. F. Parsons, A. Mazurenko, C. S. Chiu, G. Ji, D. Greif, and M. Greiner, Science **353**, 1253 (2016).
[49] M. Boll, T. A. Hilker, G. Salomon, A. Omran, J. Nespolo, L. Pollet, I. Bloch, and C. Gross, Science **353**, 1257 (2016).
[50] L. W. Cheuk, M. A. Nichols, K. R. Lawrence, M. Okan, H. Zhang, E. Khatami, N. Trivedi, T. Paiva, M. Rigol, and M. W. Zwierlein, Science **353**, 1260 (2016).